Surface plasmon-enhanced amorphous-silicon-nitride light emission with single-layer gold waveguides

Keyong Chen (陈可勇), Xue Feng (冯 雪)*, and Yidong Huang (黄翊东)

State Key Laboratory of Integrated Optoelectronics, Department of Electronic Engineering, Tsinghua University, Beijing 100084, China

**Corresponding author: x-feng@tsinghua.edu.cn*

Received August 29, 2012; accepted September 12, 2012; posted online December 25, 2012

Surface-plasmon (SP) enhancement of amorphous-silicon-nitride (a-SiN_x) light emission with single-layer gold (Au) waveguides is experimentally demonstrated through time-resolved photoluminescence measurement. The a-SiN_x active layer with strong steady-state photoluminescence at 560 nm is prepared by plasma-enhanced chemical vapor deposition, and the Au waveguide on the top of the a-SiN_x layer is fabricated by magnetron sputtering. The maximum Purcell factor value of ∼3 is achieved with identified SP resonance of the Au waveguide at ∼530 nm.

OCIS codes: 240.0240, 240.6680.

doi: 10.3788/COL201311.022401.

Silicon light emitters have attracted great attention due to the compatibility of optoelectronic integration with the standard complementary metal oxide semiconductor (CMOS) processes[1,2]. In order to achieve practical silicon light emitters, various nano-structured silicon materials, including porous silicon, silicon oxide (SiO_x) and silicon nitride (SiN_x), have been proposed and demonstrated[3−8]. However, the emission efficiency of such materials is still much lower than that of III-IV semiconductors[9−14]. Surface plasmon (SP) is a promising way to improve spontaneous emission (SE), due to its large density of states for photons and the small mode volume of the electromagnetic field (i.e., SP mode). In our previous work, several approaches have been proposed for SP-enhanced Si light emitters, including single/double-layer metal waveguide, cermet waveguide, and metallic grating[15−19]. In the current work, the single-layer metal waveguide approach is experimentally demonstrated with the active material of SiN_x. We adopted SiN_x due to its lower potential barriers compared with SiO_x; this characteristic facilitates the carrier injection of electrically-pumped devices. A gold (Au) waveguide is fabricated on top of the SiN_x active layer by magnetron sputtering, after which the SP enhancement is evaluated through time-resolved photoluminescence (TRPL) measurement. The maximum value of measured Purcell factor (PF) is ∼3.

In our experiments, the steady-state photoluminescence (SSPL) and TRPL measurements were performed using a photoluminescence spectrometer (FLSP920, Edinburgh Instrument) equipped with a 450-W steady state xenon lamp (Xe900) and a nanosecond flash lamp (nF900). Firstly, a series of amorphous-silicon-nitride (a-SiN_x) samples with different SSPL peaks in the range of 450 to 700 nm were prepared on the silicon substrates. This process was completed by plasma-enhanced chemical vapor deposition (PECVD, L-450P CVD System, Anelva), using SiH_4 and NH_3 or N_2 as the reactant gas sources. The measured SSPL spectra at the excitation wavelength of 325 nm for the three typical samples (A to C, respectively) are shown in Fig. 1, and their deposition conditions are given in Table 1. The difference in emission peaks of a-SiN_x may arise from amorphous silicon nano-clusters with varied average sizes of <3 nm[20,21]. In principle, the central emission wavelength of SiN_x should be consistent with the SP resonance wavelength of Au (∼530 nm) in order to achieve the maximum SE enhancement. However, in order to distinguish the SP resonance from original SSPL, sample B with the SSPL peak at 560 nm was utilized to demonstrate the emission peak caused by the SP resonance. Although such arrangement can lead to the deterioration of the PF, it is helpful in identifying the SP resonance. The refractive index of sample B was measured to be 1.99 at 630 nm by an ellipsometer. Subsequently, a thin Au film was sputtered on the top of the a-SiN_x sample with Au target (99.99%) and pure

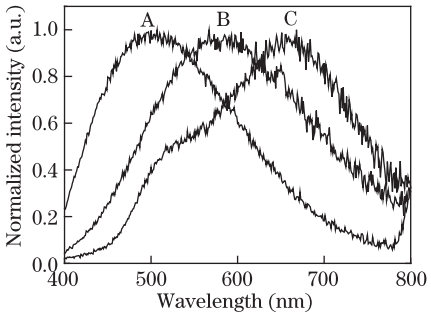

Fig. 1. SSPL of three different plasma-enhanced chemical vapor deposited a-SiN_x samples from A to C at the excitation wavelength of 325 nm.

Table 1. PECVD Conditions of a-SiN_x Samples

#	SiH_4 (sccm)	N_2 (sccm)	NH_3 (sccm)	Temperature (°C)	Pressure (Pa)	Power (W)
A	9	0	10	RT	25	20
B	9	0	10	300	25	20
C	4	80	0	300	70	150

Note: RT stands for room temperature.

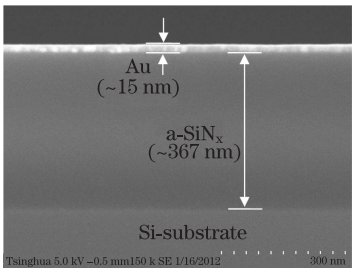

Fig. 2. Cross-sectional scanning electron microscope image of the a-SiN_x sample coated with a 15-nm-thick Au waveguide.

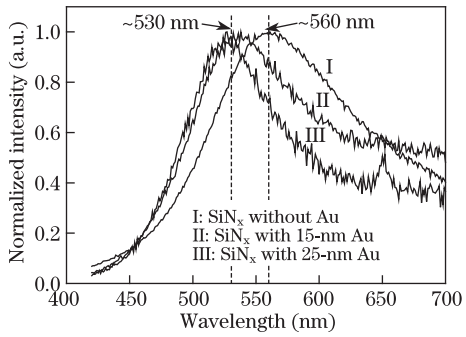

Fig. 3. SSPL of the a-SiN_x samples without and with single-layer Au waveguides (thicknesses of 15 and 25 nm, respectively) at the excitation wavelength of 325 nm.

Argon gas (99.999%). Figure 2 shows the cross-sectional scanning electron microscope (SEM, S-5500, Hitachi) image of sample B with thickness of ~367 nm and coated with a 15-nm-thick Au waveguide. For comparison, the same a-SiN_x sample with a 25-nm-thick Au waveguide was also prepared.

Then, the SSPL spectra of all the samples (without/with single-layer Au waveguides) were measured while the excitation light with the wavelength of 325 nm was incident from the Au-coating side (Fig. 3). Here, the spectra were normalized to recognize the peak positions. Given that the excitation light is partly reflected outside by the Au films, the measured SSPL intensities of the coated samples are much lower than that of the uncoated one. In addition, the peak wavelength of the uncoated sample is 560 nm, whereas the SSPL peak wavelengths of the coated samples with 15 and 25 nm Au are almost the same as 530 nm (Fig. 3). For a deeper insight, the density of states (DOS) of each coated sample was calculated based on the formula of $\mathrm{d}(\beta^2)/\mathrm{d}(\hbar\omega)$. In this formula, β is the propagation constant, $\hbar$ is the reduced Planck's constant, and ω is the angular frequency[17]. The maximum DOS values of both Au waveguides are the same (~2.2 eV), and are very close to the measured SSPL peak position (~530 nm/~2.3 eV) of the coated samples (Fig. 4). Meanwhile, the SP resonance can be red-shifted by increasing the ambient effective refractive index above the Au waveguide; this can be achieved by coating it with a higher index material and/or increasing its thickness[16]. A thin Si film was sputtered on the 15-nm-Au-coated sample with Si target (99.99%) in order to observe the peak shift. By increasing the Si thickness from ~15 to ~30 nm, the SSPL peak position of the coated sample is red-shifted to the original one (560 nm) of the uncoated sample (Fig. 5). The inset of Fig. 5 is the cross-sectional SEM image of the coated sample with 30-nm Si and 15-nm Au layers. Therefore, it is reasonable that the measured SSPL peaks around 530 nm originate from the SP resonance of the Au waveguides.

In order to evaluate the SP enhancement, photoluminescence (PL) lifetimes of all the samples were measured with TRPL. The PF can be calculated with the definition of $\mathrm{PF}=\tau/\tau^*$, in which τ is the original PL lifetime and τ^* is the enhanced one[22]. Figure 6 shows the TRPL spectra (thin line) with the fixed excitation/detection wavelength of 325 nm/560 nm. The fitted curves using the following double exponential function (thick line) were also plotted[23]. The function is given as

$$R(t) = a_0 + a_1 \mathrm{e}^{-t/\tau_1} + a_2 \mathrm{e}^{-t/\tau_2}, \tag{1}$$

where τ_1 and τ_2 are the two dominant decay times representing the recombination of electron-hole pairs (excitons) with two different lifetimes of around one and a few nanoseconds in a-SiN_x, respectively, a_1 and a_2 are the pre-exponential factors, and a_0 is the additional background. The descending edges of the fitted curves for both coated samples are steeper than those of the uncoated sample, indicating decreased PL lifetimes or the improved spontaneous emission rates. With the measured values of τ_1 and τ_2, the average lifetime (τ_{ave}) can be calculated through the following equation:

$$\tau_{\mathrm{ave}} = b_1\tau_1 + b_2\tau_2, \tag{2}$$

where b_1 and b_2 are the relative PL intensities ($a_i\tau_i/(a_1\tau_1 + a_2\tau_2) \times 100\%, i = 1\,\mathrm{or}\,2$) of the first and

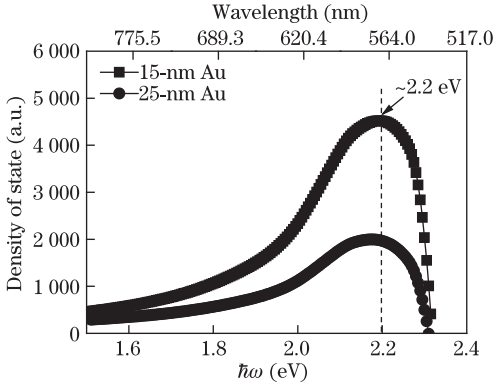

Fig. 4. Calculated density of states of both coated a-SiN_x samples with single-layer Au waveguides with thicknesses of 15 and 25 nm, respectively.

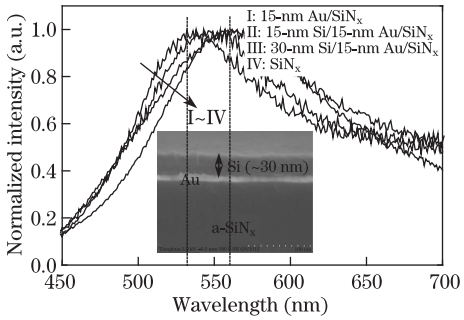

Fig. 5. SSPL of the samples of 15-nm Au/a-SiN_x (I), 15-nm Si/15-nm Au/a-SiN_x (II), 30-nm Si/15-nm Au/a-SiN_x (III), and a-SiN_x (IV). Inset: cross-sectional scanning electron microscope image of the 30-nm Si/15-nm Au/a-SiN_x sample.

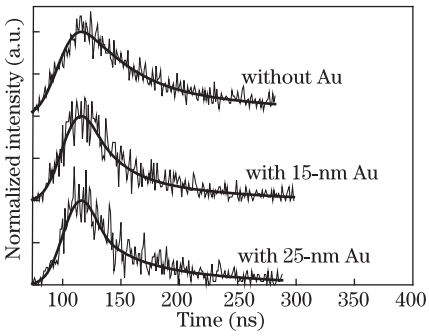

Fig. 6. TRPL (thin line) and corresponding fitted curves (thick line) of the a-SiN_x samples without and with single-layer Au waveguides (thicknesses of 15 and 25 nm, respectively) at the excitation wavelength of 325 nm and the detection wavelength of 560 nm.

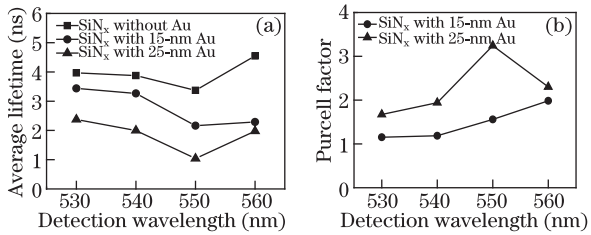

Fig. 7. (a) Average lifetimes and (b) corresponding Purcell factors of the a-SiN_x samples without and with single-layer Au waveguides (thicknesses of 15 and 25 nm, respectively), at the fixed excitation wavelength of 325 nm and different detection wavelengths of 530 to 560 nm.

second exponential components as a percentage, respectively. The average PF can be obtained by dividing the average lifetime of the uncoated sample (τ) by that of the Au-coated sample (τ^*). The calculated average lifetimes and the PFs are plotted in Fig. 7, with varied detection wavelengths ranging from 530 to 560 nm. The average lifetimes of the coated samples are shorter, and the corresponding PFs range from 1.2 to 3.2. In addition, a little larger PF is achieved with the thicker coating (25 nm) (Fig. 7(b)), though our simulation results indicate that the DOS and the corresponding PF with the thicker coating would be smaller than those with the thinner coating. Such disparity between the experimental and calculated data has yet to be explained, and the reason behind it remains unclear. At present, we are still working on the possible (joint) influence of metal waveguide properties, including thickness, surface morphology and crystalline state to the SP enhancement. However, according to the experimental results, the SP enhancement of single-layer Au waveguides for the Si light emitter can be verified when the maximum PF value of ∼3 is achieved. Considering the propagation loss of the SP mode on the smooth waveguide, the PF can be further enhanced by adopting rough waveguides to scatter SP modes into free space before significant depletion[15].

In conclusion, we fabricate a series of a-SiN_x samples through PECVD with strong SSPL in the range of 450 to 700 nm. Based on the selected sample with the SSPL peak wavelength of 560 nm, the SP resonance of Au at ∼530 nm is experimentally demonstrated through the SSPL measurement. Furthermore, the SP enhancement of single-layer Au waveguides for the a-SiN_x spontaneous emission is observed through the TRPL measurement, and the maximum PF value of ∼3 is obtained. The experimental results indicate that metal waveguides can serve as simple alternatives in improving the SE of Si light emitters.

This work was supported by the National Basic Research Program of China (Nos. 2011CBA00608 and 2011CBA00303) and the National Natural Science Foundation of China (Nos. 61036011 and 61036010).

References

1. L. Pavesi, Advances in Optical Technologies **2008,** 416926 (2008).
2. Z. Z. Yuan, A. Anopchenko, N. Daldosso, R. Guider, D. Navarro-Urrios, A. Pitanti, R. Spano, and L. Pavesi, Proc. IEEE **97,** 1250 (2009).
3. A. Marconnet, M. Panzer, S. Yerci, S. Minissale, X. Wang, X. Zhang, L. D. Negro, and K. E. Goodson, Appl. Phys. Lett. **100,** 051908 (2012).
4. S.-Y. Seo, K.-S. Cho, and J. H. Shin, Appl. Phys. Lett. **84,** 717 (2004).
5. M. Wang, A. Anopchenko, A. Marconi, E. Moser, S. Prezioso, L.Pavesi, G. Pucker, P. Bellutti, and L. Vanzetti, Phys. E **41,** 912 (2009).
6. J. Warga, R. Li, S. N. Basu, and L. Dal Negro, Appl. Phys. Lett. **93,** 151116 (2008).
7. D. Y. Song, E.-C. Cho, G. Conibeer, Y.-H. Cho, Y. D. Huang, S. J. Huang, C. Flynn, and M. A. Green, J. Vac. Sci. Technol. B **25,** 1327 (2007).
8. B. Gelloz, A. Kojima, and N. Koshida, Appl. Phys. Lett. **87,** 031107 (2005).
9. B. Gelloz and N. Koshida, J. Appl. Phys. **88,** 4319 (2000).
10. R. J. Walters, R. I. Bourianoff, and H. Atwater, Nature Mater. **4,** 143 (2005).
11. M. Peralvarez, C. Garcia, M. Lopez, B. Garrido, J. Barreto, C. Dominguez, and J. A. Rodriguez, Appl. Phys. Lett. **89,** 051112 (2006).
12. K. S. Cho, N.-M. Park, T.-Y. Kim, K.-H. Kim, G. Y. Sung, and J. H. Shin, Appl. Phys. Lett. **86,** 071909 (2005).
13. M. E. Castagna, S. Coffa, M. Monaco, A. Muscara, L. Caristia, S. Lorenti, and A. Messina, Res. Soc. Symp. Proc. **770,** I2.1.1 (2003).
14. O. Jambois, J. Carreras, A. Pérez-Rodríguez, B. Garrido, C. Bonafos, S. Schamm, and G. B. Assayag, Appl. Phys. Lett. **91,** 211105 (2007).
15. X. L. Hu, Y. D. Huang, W. Zhang, and J. D. Peng, Appl. Phys. Lett. **89,** 081112 (2006).
16. X. Tang, Y. D. Huang, Y. X. Wang, W. Zhang, and J. D. Peng, Appl. Phys. Lett. **92,** 251116 (2008).
17. X. Tang, Y. X. Wang, W. W. Ke, X. Feng, Y. D. Huang, and J. D. Peng, Opt. Commun. **283,** 2754 (2010).
18. X. Feng, F. Liu, and Y. D. Huang, Opt. Commun. **283,** 2758 (2010).
19. X. Feng, F. Liu, and Y. D. Huang, J. Lightwave Technol. **28,** 1420 (2010).
20. H.-S. Kwack, Y. P. Sun, and Y.-H. Choa, Appl. Phys. Lett. **83,** 2901 (2003).
21. B.-H. Kim, C.-H. Cho, T.-W. Kim, N.-M. Park, G. Y. Sung, and S.-J. Park, Appl. Phys. Lett. **86,** 091908 (2005).
22. K. Okamoto, I. Niki, and A. Scherer, Appl. Phys. Lett. **87,** 071102 (2005).
23. L. B. Ma, R. Song, Y. M. Miao, C. R. Li, Y. Q. Wang, and Z. X. Cao, Appl. Phys. Lett. **88,** 093102 (2006).